Experimental investigation of plasma-broadened hydrogen Balmer lines at low electron densities

H. Ehrich* and D. E. Kelleher
Institute for Basic Standards, National Bureau of Standards, Washington, D. C. 20234
(Received 14 February 1978; revised manuscript received 20 August 1979)

The central regions of the plasma-broadened Balmer lines H_α, H_β, and H_γ have been measured in a wall-stabilized arc over an electron density range between approximately 4×10^{14} and 2×10^{16} cm^{-3}. The experimental profiles exhibit much less structure in the line core than predicted by theories based on the static-ion approximations. These discrepancies increase towards lower electron densities and lower Balmer-series members, e.g., the H_α half-width as well as the central minimum of H_β deviate by about a factor of three from current hydrogen-broadening theories at low electron densities (10^{-5} cm^{-3}). Consistent with earlier experiments, the central minimum of H_β was found to depend on the reduced mass of the radiator-ion perturber system. Also, the temperature dependence of the experimental data suggests that the central H_β minimum depends approximately linearly on the relative mean velocity between radiator and perturber. Extrapolation of the H_β results to the static case yields good agreement with the quasistatic calculations. The theoretically predicted "shoulder" in the H_γ line shape is nearly absent in the experimental profile. Besides ion dynamics, fine-structure (spin) effects can account for a considerable portion of the observed discrepancies in the case of H_α, and possibly a small part in the case of H_β at low electron densities ($\lesssim10^{15}$ cm^{-3}).

I. INTRODUCTION

Calculations based on a generalized impact approximation performed by Kepple and Griem[1] (KG) yield line profiles showing less structure in the line centers than line profiles obtained from the "unified theory" by Vidal, Cooper, and Smith[2] (VCS). The difference between these two theories is mainly that the VCS calculations retain the upper- state–lower-state interference term, while the KG theory does not. Experimental investigations of the lower members of the Balmer series show considerable disagreement with both theories for the regions near the line centers.[3-18] In general, the calculated profiles exhibit significantly more structure than is observed experimentally. In attempting to account for the discrepancies between theory and experiment, the recent literature contains several discussions suggesting experimental as well as theoretical reasons for this disagreement. The following possibilities have been considered:

(i) Neglect of time ordering: Calculations by Roszman,[19] taking into account time ordering for the unified theory, show that the inclusion of time-ordering produces some smearing of the line centers of H_α and H_β. However, this smearing is much less than that observed experimentally, and, therefore, the neglect of time ordering can explain only a minor part of the discrepancies.

(ii) Inelastic collisions: Investigations by Hill, Gerardo, and Kepple[7] show that the inclusion of contributions to the line broadening from inelastic collisions between perturbing electrons and the radiating atom give an improved agreement with experiment in the line centers of H_β, H_γ, and H_δ, but poorer agreement is obtained over the profile as a whole.

(iii) Ion-dynamic effects: The suggestion made by some authors[7,16] that the observed discrepancies are due to the breakdown of the quasistatic approximation for the ions was confirmed experimentally. It was observed by Kelleher and Wiese[15] and Wiese *et al.*[14] that the central regions of the first four Balmer lines depend significantly on the reduced mass μ in the radiator- (ion) perturber system. With increasing reduced mass the experimental profiles tend to approach the calculated profiles. Assuming a simple $1/\sqrt{\mu}$ dependence of the H_α half-width (this dependence was observed for the central minimum or "dip" of H_β), surprisingly good agreement with theory[19] was found by extrapolating the experimental values to the static case. This implies that the current hydrogen-broadening theories may be interpreted as a limiting case for vanishing relative radiator- (ion) perturber velocity. Ion-dynamic effects produce a further smearing of the line centers.

In contrast to these experimental results, some theoretical studies on the subject of ion dynamics in the case of hydrogen lines yield only minor effects.[10,20,21] (However, a recent calculation by Voslamber[22] for L_α predicts ion-dynamic effects which increase the width by 80%. Significant effects are also expected for Balmer lines.) H_α and H_β profiles calculated by Cooper, Smith, and Vidal[23] (CSV) show a considerable smearing of the line centers due to inclusion of ion-dynamic effects,

but the validity of these computations are restricted to electron densities below 10^{15} cm^{-3}.

(iv) Plasma inhomogeneities: In a recent experiment Hey and Griem[10] investigated the central structure of H_α and H_β (D_β) by means of an electromagnetically driven shock tube. Their obtained H_β (D_β) profiles show much less structure in the line centers than predicted by the theories. On the other hand, their measured H_β and D_β "dips" do not show any reduced mass dependence. The authors explain the discrepancies between experimental and theoretical profiles in terms of plasma inhomogeneities, i.e., the central minimum of H_β is filled in by narrow line profiles emitted from a thin end layer in the shock tube.

In this paper we report results concerning the plasma-broadened shapes of H_α (D_α), H_β (D_β), and H_γ in the electron-density region between approximately 4×10^{14} and 2×10^{16} cm^{-3}. Most of the experimental work on hydrogen line broadening has been done[3-15] at electron densities in the range between 10^{16} and 2×10^{17} cm^{-3}. Only a few experimental data exist at lower values.[16-18] If the present experiment is combined with earlier ones,[3,9,14,15] arc measurements of the first three Balmer lines are now available for nearly three orders of magnitude in electron density. This wide range of conditions affords a very critical test of Stark-broadening theories and to some extent makes it possible to distinguish between the different broadening mechanisms mentioned above. Also, at very low electron densities, hydrogen and deuterium profiles can be spectrally resolved in the same plasma due to the isotopic shift between H and D lines. This method allows a clear decision as to whether the reasons discussed in (iii) or (iv) above are responsible for the observed discrepancies in hydrogen line centers.

II. EXPERIMENT

A. Experimental setup

Figure 1 shows a schematic of our experimental setup. The light source was a wall-stabilized arc, running in pure helium with a small admixture of hydrogen and deuterium, respectively, only in the central portion of the arc length. The wall-stablized arc has been described extensively in earlier publications.[24,25] The arc used in this experiment is very similar to that described in Ref. 26; here we only give the main details. The arc channel of 3.2 mm diameter and about 70 mm length was built up from a stack of 30 water-cooled copper plates, each of them approximately 1.6 mm thick. The plates were insulated electrically from each other by means of rubber rings

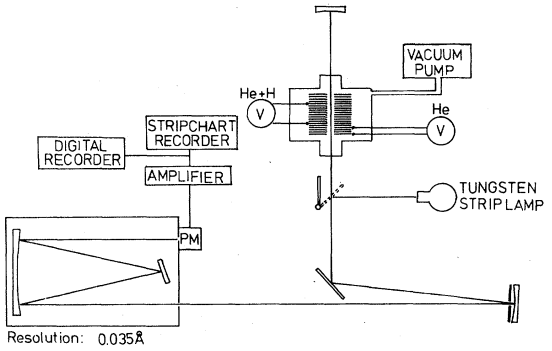

FIG. 1. Schematic diagram of the experimental setup.

producing a spacing between the plates of about 0.4 mm. This narrow spacing ensured a nearly uniform plasma column by avoiding expansion of the plasma into the space between the plates. At a few positions within the arc channel, where gas inputs and outlets were necessary, the spacing between the plates was a little wider. Anode and cathode each consisted of a set of four water-cooled tungsten electrodes. The whole arc was placed in a vacuum-tight vessel, allowing operation of the arc at low pressures with the aid of a vacuum regulator. The arc was operated with a current-stabilized dc power supply; the residual current ripple was less than 0.3%, and the current stability was approximately 0.2% over many hours of running time.

We observed the arc end-on down the central axis. Because the hydrogen lines were most strongly emitted from an outer shell close to the arc channel wall, we did not make any side-on measurements due to problems with the Abel inversion. In order to avoid any end-layer effects, only the central length of the arc contained a small admixture of less than 1% atomic hydrogen, while a "plasma window" of pure helium was maintained in the electrode regions. In our helium arc a good gas separation could only be obtained under certain gas flows. Ultrapure helium entered the arc channel from both ends with a high flow and came out between two cascade plates in the arc center. A mixture of 98% He and 2% H_2 was added to the helium flow approximately 10 mm above and below the central region of the arc channel. The voltage across the arc plates turned out to depend very sensitively on the hydrogen admixture to the pure helium arc. By measuring the voltage across the central arc region containing the hydrogen admixture and across the hydrogen-free electrode regions, we were able to determine the optimal gas-flow rates for a good gas separation. During the experiment the voltage measure-

ments served as a monitor for hydrogen-free electrode regions. In the case of the low-pressure arc, a suitable gas flow was maintained by means of a throttle valve in the pumping line between the arc vessel and the vacuum pump.

The arc channel was imaged with a magnification ratio of about 2:1 onto the entrance slit of a monochromator with a spherical mirror. A small-aperture optical system (f/140) and a mask before the monochromator entrance slit ensured sufficient spatial resolution. The optical depth was checked by focusing the light passing through the back end of the arc back onto the arc axis with a spherical mirror. The whole system was calibrated by means of a tungsten strip lamp. A 2 m Czerny-Turner monochromator with a holographic 1800 lines/mm grating was used. The resolution in first order is 0.03 Å with optimal slit settings. The instrumental profiles—determined by means of a ^{198}Hg microwave discharge—were found to be closely Gaussian in the line core, but somewhat shallower in the line wings. The line profiles were recorded photoelectrically with a strip-chart recorder or, where necessary, a digital recorder which allowed for storing the data on tape for further computer analysis.

B. Line-profile measurements

The results of this experiment as well as the plasma analysis are based on line-shape measurements. In order to avoid systematic errors in the obtained results, the following factors entering into the line-profile measurements have been considered.

(i) Homogeneity of the observed plasma region. We checked spectroscopically for plasma inhomogeneities by observing the shape of the lines He *I* 5016 Å and H_β, respectively. The helium line is broadened as well as blue-shifted by the plasma. A profile emitted from an inhomogeneous plasma layer exhibits an asymmetry, enhancing the red wing over the blue one, because emission from plasma layers of relatively low electron density mainly contributes to the intensity of the red line wing in the observed profile. In our arc the above-mentioned helium lines showed a distinct asymmetry, which could be removed by introducing neon instead of helium into the electrode regions, while a helium plasma was maintained only in the arc center. In this case the helium line showed a much smaller asymmetry of opposite direction, namely, enhancing the blue over the red wing in agreement with theoretical predictions[27,28] and experimental results. (See, for example, Ref. 29.)

We concluded from this that end-layer effects in our arc would cause significant errors in line-profile measurements, but that, if the end layers are removed by a suitable plasma window, the observed plasma column containing the study gas in the arc center is homogeneous.

Figure 2 demonstrates the influence of plasma inhomogeneities on the central structure of H_β. Figure 2(a) shows an H_β profile emitted from a homogeneous plasma layer. Whenever a very small amount of hydrogen was allowed to enter the "helium window," dramatic changes occurred in the H_β line center as can be seen in Fig. 2(b). The central dip is filled in by the relatively narrow line emitted from low-electron-density regions, and simultaneously the asymmetry, which is hardly detectable in Fig. 2(a), increases significantly. This enlargement of the asymmetry is due to the red shift[3] of the main body of the H_β profile with respect to the narrow line profiles emitted from low-electron-density regions; this effect increases the blue peak more than the red one. Hydrogen impurities in the electrode regions producing profiles like that shown in Fig. 2(b) were clearly detectable by means of the voltage measurements across arc plates. H_β profiles like that shown in Fig. 2(a) were only obtained when the voltage across the electrode regions remained exactly unchanged after introducing hydrogen and deuterium, respectively, to the center of the helium arc. Thus, the well-known structure of the H_β line center can serve as a very sensitive homogeneity monitor.[30]

(ii) Stability of the plasma conditions. This was checked at the beginning and repeatedly during each experimental run by monitoring the intensity at certain wavelength positions in the center of helium and hydrogen (deuterium) lines as well as by H_β (D_β) half-width measurements. After a "warm-up time" of as long as several hours, no systematic trends could be observed, and the scatter in the obtained values lay typically within ±1%. This stability of our arc source (and the

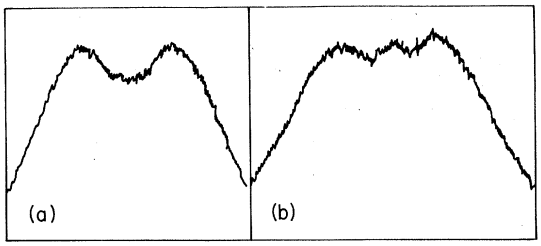

FIG. 2. (a) H_β line center emitted from homogeneous plasma layer (b) H_β line center emitted from inhomogeneous plasma layer; the dip is filled up by narrow line profiles produced in cold end layers. The asymmetry is enhanced by the red shift of the main body.

photoelectric registration equipment) enabled a long time integration of the signals and allowed an excellent signal-to-noise ratio.

(iii) Optical depth. Emission of the investigated line profiles from an optically thin plasma layer was confirmed directly by focusing the light passing through the rear end of the arc back onto the arc axis. The optical depth τ can be obtained from

$$\tau_\lambda = \ln[(A-1)/(B_\lambda - 1)], \quad (1)$$

where A is the ratio of the signals with and without the reflected light included, measured at an optically thin wavelength (e.g., line wing), and B_λ is this ratio at a wavelength λ where τ is desired. By adjusting the concentration of the study gas in the arc center, the optical depth in the line peaks was always kept below 0.02. Therefore, no corrections were necessary.

Very often the optical depth is determined by comparing the absolute intensities of the line peaks $I(\lambda, T)$ with those of a blackbody $B(\lambda, T)$ at the plasma temperature T:

$$I(\lambda, T) = B(\lambda, T)[1 - \exp(-\tau)]. \quad (2)$$

For small optical depths ($\tau \ll 1$), one obtains

$$\tau = I(\lambda, T)/B(\lambda, T). \quad (3)$$

However, this method is only applicable in the case of local thermodynamic equilibrium (LTE).[31] In the case of a non-LTE plasma, if radiation from only one line is significant, i.e., continuum and other line radiation are negligible, the temperature in the Planck function

$$B(\lambda, T) = (2hc^2/\lambda^5)[\exp(hc/\lambda kT) - 1]^{-1} \quad (4)$$

is the population temperature for the energy levels of this particular line (h, c, and k are the usual constants). Replacements of the exponential in (4) by the Boltzmann distribution

$$n_1/n_2 = (g_1/g_2)\exp(hc/\lambda kT) \quad (5)$$

leads to the source function

$$S(\lambda, T) = \left(\frac{2hc^2}{\lambda^5}\frac{g_1 n_2}{g_2 n_1} - 1\right)^{-1}; \quad (6)$$

n_1 and n_2 are the population densities of the lower and upper states of the considered line, and g_1 and g_2, their statistical weights. In the case of a non-LTE plasma,[31] the value of the source function, which gives the blackbody limit for a particular line, can be considerably lower than the value of the Planck function based on an experimentally obtained "plasma temperature." Especially, resonance lines or transitions ending on a metastable state should be treated with caution due to overpopulation of the lower state. In the present experiment we found significant deviations from LTE and, therefore, the optical depth was always measured directly as described above.

(iv) Background under the lines. In order to obtain the real line shape, the background has to be subtracted from a recorded line profile. At the beginning of each run, the spectrum of the pure-helium arc was recorded in the wavelength regions where lines were desired to be measured. The underlying continuum intensity generally turned out to be very constant, and thus—after introducing the study gas into the arc center—the background could readily be obtained from the continuum level on both sides of the lines. At higher electron densities, the wings of the lines He I4922 and 4388 Å had to be taken into account in the H_β and H_γ line-shape measurements. Due to overlapping with the helium line, the H_γ measurements were restricted to electron densities below 8×10^{15} cm^{-3}.

(v) Experimental setup and instrumentation. We paid particular attention to the following aspects of our instrumentation: exact alignment of the arc, linearity of the photoelectric registration equipment, possible changes in the spectral sensitivity of the photomultiplier within one line profile (which were negligible), calibration of the scanning rate of the spectrometer, prevention of interference and fluorescence effects in windows and optical filters, sufficient instrumental resolution including the time constant of the registration equipment, and calibration of the whole system by means of a tungsten strip lamp. Besides these factors of general interst, other factors concerning special lines will be discussed later.

C. Plasma analysis

In this section we report the diagnostic methods and results for the determination of the plasma parameters.

(i) Electron temperature. As will be shown in the following, strong deviations from LTE are present in our helium arc; e.g., the electron temperature is much higher than the gas temperature. Therefore, one has to consider first of all what temperature is important for the present investigations. The usual line-broadening theories for hydrogen[1,2] treat the ions statically; only the velocity of the electrons, i.e., the kinetic electron temperature, enters the calculations. Since the calculated profiles depend rather weakly on the electron temperature, this physical quantity is not a very critical factor in our case. We determined the electron temperature from the intensity ratio of the argon lines A II 4348 Å/A I 8115 Å assuming LTE population of the argon states. For this purpose trace amounts of argon were introduced into the arc center. The influence of the

very small argon admixture on the helium plasma was checked by monitoring the intensity of line He I 5016 Å. After introducing the argon into the arc, the intensity of the helium line was found to be approximately 3% lower, and thus the disturbance of the helium plasma was minor. Though deviations from LTE in the population of the argon excited states are possible, these LTE deviations should cause relatively insignificant errors in the electron temperature. Since the argon intensity ratio depends very steeply on the electron temperature, even strong deviations from an LTE population of, for example 100% would only cause an error in the measured value of about 1000 K (5%–7%).

(ii) Gas temperature. The kinetic temperature of the neutral atoms and ions (both species are assumed to have the same temperature, which is called here gas temperature) can be obtained by means of the Doppler width of a suitable spectral line, if a Maxwellian velocity distribution exists. In this experiment we determined the gas temperature from the Doppler width of the Ne I 6402-Å line. For this purpose trace amounts of neon were added to the arc center. For our experimental conditions Doppler broadening of this line dominates all other broadening mechanisms. In order to obtain the pure Doppler width, the other broadening effects had to be taken into account. The influence of the instrumental resolution was kept small by using the 2-m Czerny-Turner monochromator with an apparatus function close to a Gaussian profile, having a full width at half maximum of 0.035 Å for our slit settings. The measured neon lines showed a Voigt profile arising from a convolution of a Gaussian (Doppler and instrumental broadening) and a dispersion profile (Stark and neutral-atom braodening). A deconvolution procedure was performed by applying a Voigt profile analysis (see Ref. 32), from which we obtained the Gaussian as well as the dispersion part of the measured profile. Subtraction (difference of squares) of the instrumental broadening from the Gaussian part finally led to the pure Doppler width.

This deconvolution procedure was checked in the following way: we added small amounts of neon to the center of an *argon* arc. At the electron densities produced in this arc (near 10^{17} cm^{-3}), the neon line mentioned above is primarily Stark broadened; the obtained Stark half-width agreed quite well with values calculated by Griem.[1(b)] The half-widths of the dispersion profile contained in the Voigt profiles were only slightly larger than one would expect from these results, showing that the major portion in the dispersion part is caused by Stark broadening of the neon lines. The additional small broadening (10–20 mÅ) is partly due to Van der Waals broadening (~7 mÅ) by neutral helium atoms.

In the analysis of our results, we assume that the temperature of the trace hydrogen atoms as well as the helium atoms and ions have the same temperature as that determined from the trace neon atoms. One might question the validity of this assumption for hydrogen on the grounds that the dissociation of H_2 produces hydrogen atoms with extra kinetic energy. Dissociation occurs via excited molecular states which, in the Franck-Condon region above the ground state, have an energy greater than that required for dissociation. This extra energy turns up as kinetic energy of the resultant atoms. For example, an energy of about 8.8 eV is required to excite the repulsive $1^3\Sigma_u$ state from the H_2 ground state. Since the H_2 dissociation energy is only 4.5 eV, each H atom departs with an extra kinetic energy of 2.2 eV. According to Massey and Burhop,[33] this is one of the more important dissociation mechanisms.

In the following we wish to demonstrate that the temperature of the hydrogen atoms we observe is very close to that of the other heavy particles in the plasma. The energy threshold for "dissociative excitation," which yields excited atoms directly, is too high for this process to be significant in our cool plasma. Dissociation into the ground state predominates, and at our plasma conditions these atoms equilibrate before they are excited. At very low electron densities we could check the validity of this more directly. A comparison of the widths of H_α and D_α allows us to put an upper limit on the H ($n=3$) temperature. This temperature is only 10% greater than that deduced from the Doppler temperature of a neon line. In the following discussion, we consider each of these points in more detail.

The threshold for dissociation leaving one of the atoms in the $n=3$ state is 17 eV (4.4 for separating the nuclei plus 12.6 for the $n=3$ excitation). In a recent review of dissociative excitation of H_2, Glass-Manjean[34] points out that "slow" atoms of about 0.42 eV kinetic energy are produced by electron impact in the 19–25-eV incident energy range via predissociation. Above 25 eV, "fast" atoms of 4 to 8 eV kinetic energy are formed from doubly excited repulsive states. Considering that the effective threshold for dissociation directly into the $n=3$ state is about 19 eV, and about 8.8 eV for neutral products, dissociation into the ground state is thus about $\exp(19-8.8)/1.5$ or 10^3 times as important in a plasma with 1.5-eV electrons. Also, in this weakly ionized plasma we can ignore dissociative recombination.

Thus the dominant mechanism for generation of $n=3$ hydrogen atoms is dissociation via electron

collisions into the ground state and subsequent excitation to $n=3$. The rate for electron excitation can be approximated from the work of Gryzinski[35]:

$$k(n=1\rightarrow 3)=4.6\times10^{-9}\exp\left(\frac{-12.09}{kT_e}\right)\ \text{cm}^2\ s^{-1}.$$

At an electron temperature of 1.5 eV and an electron density of 10^{15} cm^{-3}, the rate of excitation $\nu = k N_e$ is about 10^3 s^{-1}. As we will show below, this rate of excitation from the ground state is about five orders of magnitude less than the rate at which the atoms are equilibrated.

Excitation of hydrogen neutrals by helium atoms is negligible due to the low helium-hydrogen collision rate. The helium atoms are much cooler than the electrons, in addition to being much more massive. Resonant energy exchange with metastables, which for some plasmas can also lead to anomalously high kinetic energies,[37] is unimportant in the present case because the helium metastable level is 7.6 eV above the hydrogen $n=3$ level. The mean free path (mfp) λ for a hydrogen atom in a plasma composed primarily of neutral helium is given by[36]

$$\lambda^{-1}=\pi N_{\text{He}}(R_{\text{H}}+R_{\text{He}})^2(1+m_{\text{H}}/m_{\text{He}})^{1/2}.$$

The helium density at 70 Torr, $T_g=6000\,^\circ$K is 10^{17} cm^{-3}. Using geometrical values for the radii, the mean free path of a neutral hydrogen atom in the arc is about 0.05 mm.

Energy transfer in a hydrogen-helium collision is relatively efficient. For a gas with two particles of mass m and M, temperature T_m and T_n, respectively, the fractional energy loss is[36]

$$\Delta=\tfrac{8}{3}[mM/(m+M)^2](1-T_m/T_M).$$

For $T_{\text{H}}\gg T_{\text{He}}$, $\Delta=0.43$. Thus relatively few collisions are required for equilibration. The hydrogen-helium collision frequency, $\nu=\lambda^{-1}v$, for $T=6000$ K, is about 10^8 s^{-1} or five orders of magnitude greater than the excitation rate from electrons.

We conclude that dissociated hydrogen atoms in our plasma equilibrate before radiating. This is especially the case along the central axis of the arc where our measurements were made. Most of the dissociation occurs near the radial edge of the arc, as can be seen by an outer "ring" of H_α emission. With a mfp of 0.05 mm, atomc experience many collisions before reaching the central axis.

As an experimental check on this important conclusion, we were able to determine directly an upper limit for the hydrogen temperature at very low electron densities. D_α is isotopically shifted from H_α by 1.8 Å. At electron densities below 5×10^{14}, the profiles of the two lines can be spectroscopically resolved [see Fig. 3(a)]. By

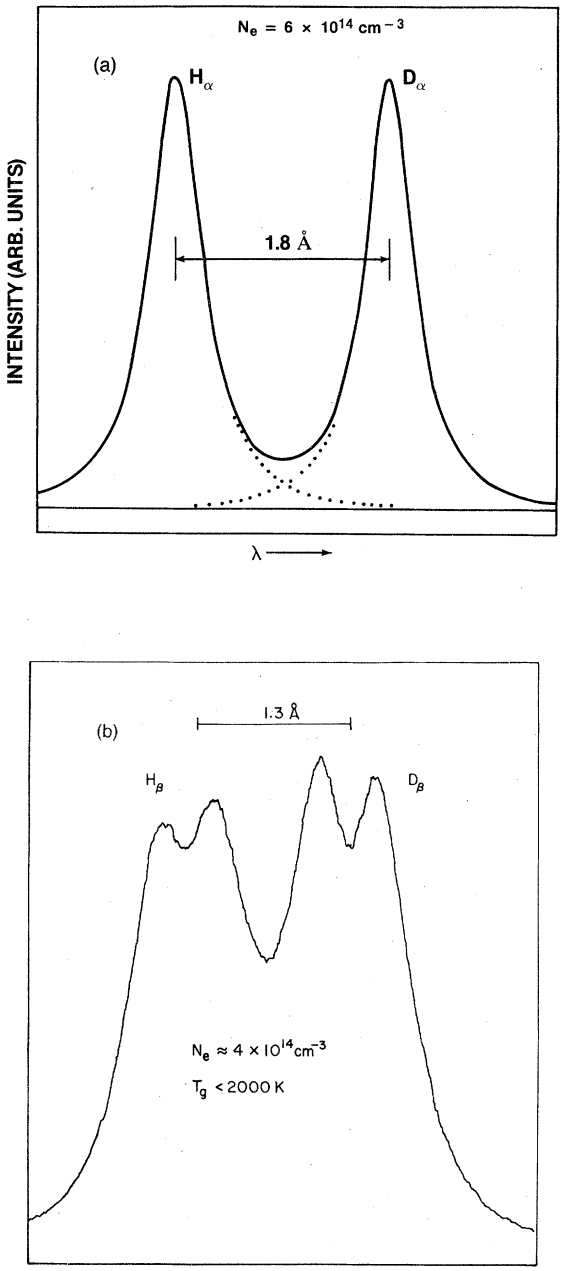

FIG. 3. (a) H_α and D_α emitted simultaneously from the same plasma at an electron density of about 4×10^{14} cm^{-3}, $T_g=2000$ K. The dotted and dashed lines indicate the separated profiles and the background. The reduced mass is 0.8 (H $-$ He$^+$) for H_α and 1.3 (D $-$ He$^+$) for D_α. The gas temperature required to Doppler-fold D_α to the same width as H_α was only about 10% greater than 2000 K. (b) H_β and D_β, same conditions as in (a). After separating the two profiles, the D_β profile was convolved with a Gaussian profile to give it the same Doppler width as H_β, assuming $T_g=2000$ K. The D_β profile then has the same width as H_β (0.90 Å), but its dip is 0.145, while that for H_β is only 0.087.

assuming that the difference in their widths is due entirely to Doppler broadening at $T_g = 2000$ K, we derived an upper limit to the hydrogen temperature which was on the average about 10% larger than that derived from the Doppler width of the neon line. This implies relatively small ion-dynamics effects for these conditions, which is consistent with the fact that in this case the ion temperature is about eight times lower than the electron temperature. In this case the ion collisions are much more quasistatic in nature, i.e., the electron-atom collisional lifetime is much less than the ion-atom collision duration. However, even at these conditions, the H_β-D_β dips showed a pronounced ion-dynamic effect. After the D_β profile [Fig. 3(b)] was substracted out from the H_β profile and then Doppler-folded ($T_g = 2000$ K) to have the same Doppler width as H_β, the widths of the two profiles were identical, yet the resultant dip of D_β was 0.145 while that of H_β was only 0.087.

We conclude that the kinetic temperature of the excited hydrogen atoms we observe is equal to that of the other heavy particles in the plasma, as indicated in Fig. 4.

(iii) Electron-density. The electron density was determined from the half-width of the H_β (D_β) profile using Stark-broadening tables published by Vidal, Cooper, and Smith.[2] The difference between electron and gas temperature was taken into account by convolving the tabulated profiles for the measured electron temperature (without Doppler broadening) with the Doppler profile for the measured gas temperature. Though the obtained electron density depends on the electron temperature, and vice versa, an iteration procedure did not give any further improvement, because both quantities depend very weakly on each other. The H_β profile has been widely used as a diagnostic tool for the determination of electron densities, and good agreement was found with independently determined electron densities. Recent measurements show that the error is less than 10% for $N_e \approx 10^{16}$ cm^{-3} and is possibly slightly higher at $N_e \approx 10^{15}$ cm^{-3} [Refs. (8), (16), and (34)].

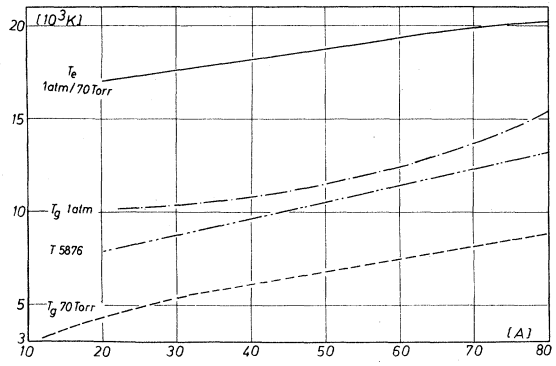

FIG. 4. Temperatures in the helium arc vs arc current for arc pressures of 1 atm and 70 torr. Electron temperature (T_e), gas temperature (T_g), and blackbody temperature of the line He I 5876 (T 5876) are very different. While T_e does not depend on the arc pressure at a fixed current, the gas temperature decreases significantly by reducing the arc pressure from 1 atm to 70 Torr. T 5876 was only determined for the 1 atm arc.

(iv) Blackbody temperature of the line He I 5876 Å. In the case of LTE, a further evaluation of the plasma temperature is possible by means of spectral lines having a measurable optical depth in the line center. As has been described in Sec. II B (iii), the value of the source function, and thus the Boltzmann $n = 2, 3$ population temperature, can be obtained if the optical depth and the absolute intensity are known at a certain wavelength. In this experiment we applied this method to the line He I 5876 Å. To minimize the influence of cold end layers causing reabsorption effects mainly in the very line center, the measurements were done at approximately three-fourths of the peak intensity on the blue side.

(v) Results. Figure 4 shows the measured temperatures plotted versus the arc current for arc pressures of 1 atm and 70 Torr. As can be seen, we obtained drastic differences between electron and gas temperatures on the one hand, and between electron temperatures and blackbody temperatures of the helium line (T 5876) on the other. While only minor changes in the electron temperature were observed by reducing the arc pressure from 1 atm to 70 Torr at a fixed arc current, the gas temperature decreased at the same time to significantly lower values. The low value of T 5876 with respect to T_e determined by means of the argon line intensity ratio (measurements were only carried out for the 1-atm arc) can be readily understood in terms of lower-level overpopulation of the helium transition according to the discussion above. Thus, this temperature does not have any further significance for the investigations of this experiment, but it gives an example of the importance of direct checks of the optical depth in a non-LTE plasma.

Extensive investigations of non-LTE effects have been carried out by Uhlenbusch *et al.*[39] These authors have published results for a 1-atm helium arc with a channel 3-mm in diameter (this experiment: 3.2 mm) operated at an arc current of 50 A. It can be seen in Table I that our measurements are in close agreement with these results obtained in a quite different manner. The range in the values of Uhlenbusch *et al.* reflects the results of

TABLE I. Comparison of measured values for electron density, electron and gas temperatures with results obtained by Uhlenbusch *et al.* (Ref. 39) for a helium arc.

Author	N_e (cm^{-3})	T_e (K)	T_g (K)
Uhlenbusch *et al.*	$(6–10)\times 10^{15}$	21 000	$(9–11)\times 10^3$
This experiment	7.8×10^{15}	19 000	11 500

different methods applied in the investigations. This agreement supports our experimental results, especially the electron temperature; our slightly lower value may be due to non-LTE effects in the population of the argon states.

For convenience in later discussion, we have plotted the measured electron and gas temperatures versus electron density in Fig. 5. In the 1-atm helium arc we were able to cover an electron-density range between 3.5×10^{15} and 2×10^{16} cm^{-3}. By running the arc at 70 Torr, an electron-density range between approximately 7×10^{14} and 4×10^{15} cm^{-3} could be spanned. Nearly all hydrogen-line measurements were carried out either in a 1-atm—or a 70-Torr—arc, and thus values for the electron and gas temperatures can be obtained from Fig. 5 at a certain electron density. A few measurements at very low electron densities were performed at about 50-Torr arc pressure (not included in Fig. 5). Note especially in Fig. 5 the overlapping regions around $N_e = 3.5\times 10^{15}$ cm^{-3}; here we were able to obtain hydrogen profiles at the same electron density, but at a different set of temperatures.

Uncertainties in the gas and electron temperatures were due mainly to non-LTE effects and the deconvolution procedure, respectively. The error

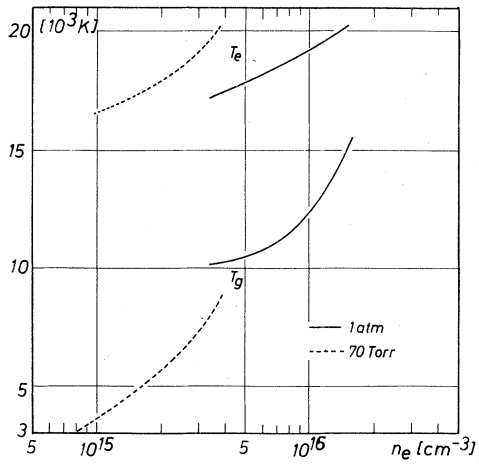

FIG. 5. Gas and electron temperatures of this experiment vs electron density.

was estimated to be about ±10% in case of the gas temperature, and we conclude a similar error for the electron temperature from Table I. Since these systematic errors affect the obtained temperatures in both the 1-atm and 70-Torr arc in the same direction, the gap in the temperatures at $n_e = 3.5\times 10^{15}$ cm^{-3} in Fig. 5, which is of some importance in later discussions, should be well established.

D. Individual line profiles

The intention of this experiment was to investigate the plasma broadening of the first three members of the hydrogen Balmer series and to compare the obtained results with recent calculations as well as other experimental investigations. In the following we discuss the obtained results for the individual line profiles.

(i) H_α. Figure 6 shows an experimental H_α profile in comparison to profiles calculated by KG[1] and VCS.[2] All profiles are area normalized to unity assuming the unmeasured wings of the experimental profile to follow a $\Delta\lambda^{-5/2}$ dependence. The calculated profiles are convolved with the Doppler and instrumental profile. The agreement between the theoretical profiles is poor, as it is between the calculated and experimental profiles, the latter being much shallower in the line core than predicted by both theories. With respect to the calculations, intensity in the observed profile is mainly "transferred" from the very line center to the near line wings, while good agreement is found with the VCS calculations in the line wings. The higher wing intensity of the KG theory is outside our experimental error bars and consistent with earlier experimental investigations at higher electron densities.[3,12] In the far wings, both the experimental and VCS profile follow a $\Delta\lambda^{-5/2}$ slope.

The discrepancies in the line center indicate

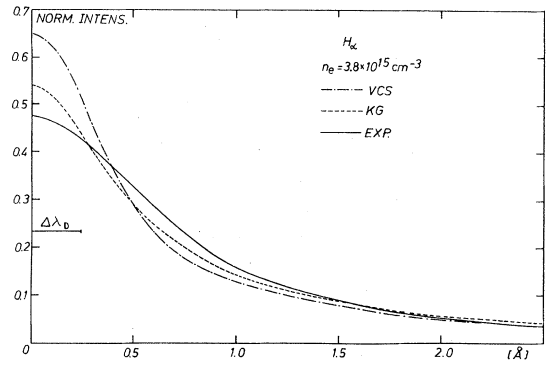

FIG. 6. Experimental and theoretical H_α profiles. The temperatures are T_e = 18 000 K and T_g = 10 200 K. $\Delta\lambda_D$ is the (half) Doppler half-width. All profiles are area normalized; the calculated profiles are convolved with the Doppler and instrumental profiles.

that there are probably some problems in the calculations with the unshifted central Stark component, which dominates strongly in the core of H_α. Including earlier arc experiments[3,9] H_α measurements are now available in the electron density range between 7×10^{14} and 10^{17} cm^{-3}. Figure 7 shows the overall situation, expressed in terms of the H_α half-width. The present experiment extends the earlier arc measurements to low electron densities, and a good agreement in the overlapping region at $N_e \approx 1.3\times10^{16}$ cm^{-3} can be seen in Fig. 7. The H_α half-widths obtained in the 70-Torr arc are somewhat smaller than those obtained from the 1-atm arc in the overlapping electron density region around $N_e = 3.5\times10^{15}$ cm^{-3}. This difference is due at least in part to the different plasma temperatures in the two arcs (see Fig. 5); the higher electron temperature as well as the lower gas temperature (Doppler effect, ion dynamics) in the low-pressure arc cause a slight narrowing of the line profile.

In order to make a reasonable comparison with theory, we corrected the measured H_α half-widths for Doppler and instrumental broadening. This was performed assuming that the H_α profiles at low electron densities have nearly the same shape as those obtained at higher densities, where non-Stark broadening effects are negligible. H_α Stark profiles with a known shape were convoluted with the Doppler and instrumental profiles. This procedure led to the measured profile for a certain Stark half-width and, thus, to an estimation of the pure Stark half-width of H_α at low electron densities. The hatched area in Fig. 7 indicates the pure H_α Stark half-width and includes the estimated uncertainty due to errors in the gas temperature and in the deconvolution procedure.

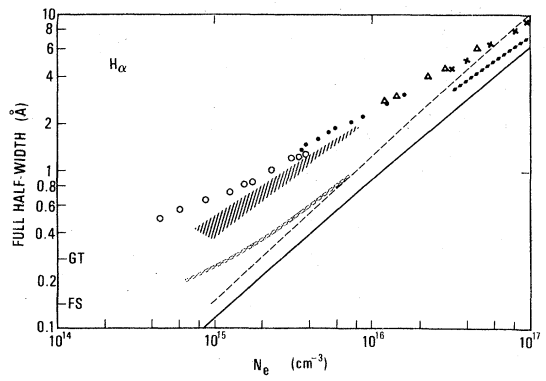

FIG. 7. Full half-width of H_α vs electron density. The curves (-----, KG; ——, VCS) show the calculated Stark half-widths without Doppler and instrumental broadening. The symbols indicate the following arc experiments: ○ and ●, this experiment (helium arc at 70 Torr and 1 atm, respectively); ×, Wiese *et al*, (Ref. 3); Δ, Ehrich and Kusch (Ref. 9). The hatched area indicates the estimated experimental half-width without Doppler and instrumental broadening. GT is the H_α half-width determined by means of a Geissler tube and FS is the wavelength distance between the two strongest fine-structure components. ◆◆◆, results of Roszman (Ref. 19) using a time-ordered unified theory for the electrons. ⧓⧓⧓, result of a weighted superposition of Lorentzian profiles at each FS component, each profile having a half-width given by the KG theory.

The curves in Fig. 7 show the pure Stark half-widths of H_α calculated by KG and VCS, respectively, for our experimental electron temperature. In regions where measurements with different electron-temperature overlap, we averaged the slightly different theoretical values for clearness in the graphs. As can be seen in Fig. 7, the discrepancies between the theories and experiment increase significantly towards low electron densities; at $N_e = 10^{15}$ cm^{-3} the experimental half-width is approximately three times larger than predicted theoretically.

In a recent paper[10] Hey and Griem report good agreement between electron densities obtained from the profiles of H_α and H_β if the KG theory is applied. This shock-tube experiment covers an electron-density range between 6×10^{16} and 1.6×10^{17} cm^{-3}, and inspection of Fig. 7 shows that these results are consistent with the earlier arc measurements at higher electron densities. The good agreement between experiments and KG theory, however, is obviously restricted to just this density range and appears to be accidental, since the theoretical curve seems to overlap the experimental data points at $N_e \approx 7\times10^{16}$ cm^{-3}. This overlapping between KG theory and experiment is also clearly visible in the data of Hey and Griem (Table V, p. 179 Ref. 10). Thus, the present results obtained at lower electron densities are not in contradiction to the measurements of these authors, but these measurements may lead to the misleading conclusion that there exists a general consistency between experiment and KG theory for H_α.

By means of Fig. 7, we are now able to explain why the peak of the experimental H_α profile in Fig. 6 lies below both theoretical line peaks, while it was observed to lie between the VCS and KG values in higher-density arc measurements.[3,14] This fact is due to the different slopes of the H_α half-width versus electron density in Fig. 7, the experimental slope being shallower than the theoretical ones. Therefore, the peaks of the area-normalized calculated profiles increase more strongly than the experimental H_α peak with decreasing electron density.

In order to account for the observed discrepancies between theory and experiment we considered

the following possibilities.

(a) Neglect of fine-structure (FS) splitting in the theories. This was the subject of an earlier paper,[18] to which we refer for details, but for completeness we will repeat briefly the most salient points. The fine-structure pattern of H_α consists of seven components, the wavelength distance between the two most intense lines being 0.142 Å. The H_α profile emitted by a Geissler tube (GT), for example, is decisively influenced by the H_α fine-structure pattern, which is smeared by Doppler broadening of the components. The half-width of this profile (GT) can be considered as a lower limit to the H_α half-width in a plasma if Doppler broadening corresponds to a temperature of more than about three thousand degrees. GT and FS are marked at the lower-left side in Fig. 7, and it can be seen that the H_α half-widths (which include Doppler broadening) measured in this experiment tend to approach the GT value. The pure Stark half-width (hatched area) is expected to approach the FS value towards very low electron densities. The theoretical half-widths, however, already have the same magnitude as FS at $N_e \approx 10^{15}$ cm^{-3}, and thus fine structure should significantly contribute to the line broadening of H_α, at least around and below $N_e = 10^{15}$ cm^{-3}.

(b) Neglect of ion-dynamic effects in the theories. Ion motion was found to be responsible for the observed discrepancies in the line centers of H_α, H_β, H_γ, and H_δ in recent arc experiments at higher electron densities.[14,15] Towards higher electron densities the influence of fine structure should decrease rapidly and the differences between experiment and theory are probably caused mainly by ion-dynamic effects.

(ii) H_β. Since the Stark pattern of H_β does not have an unshifted central component like H_α and H_γ, the plasma-broadened H_β profile exhibits a relative intensity minimum ("dip") in the line center. While good agreement was found in numerous investigations between experimental and theoretical half-widths, serious discrepancies have remained in the central region of the profile, the experimental dip being considerably smaller than predicted theoretically.

Figure 8 gives an example of a recorded H_β line profile for an electron density near 10^{15} cm^{-3}. The dip is defined in the usual way, where "max" is the averaged intensity of the two line peaks, the red peak being always some percent lower than the blue one, and "min" the intensity of the central minimum. The value of the observed dip in Fig. 8 is 0.17; this is considerably less than predicted by the theories. The KG as well as the VCS calculations yield an approximately three times larger value for the dip. Consistent with earlier

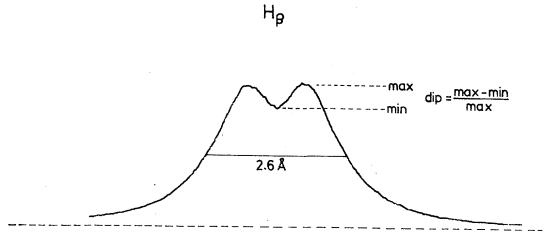

FIG. 8. Recorded H_β line profile with definition of the "dip."

arc measurements the H_β dip was found to depend on the reduced mass of the radiator- (ion) perturber system. The results are shown in Fig. 9. Introducing small admixtures of hydrogen and deuterium to the center of our helium arc, reduced masses of $\mu = 0.8$ (H – He$^+$) and $\mu = 1.3$ (D – He$^+$), respectively, were obtained. The present results are consistent with the arc measurements of Kelleher and Wiese[15] included in Fig. 9 and performed for reduced masses of $\mu = 0.5$ (H – H$^+$), $\mu = 1.0$ (H – A$^+$), and $\mu = 1.9$ (D – A$^+$): the dip deepens systematically with increasing reduced mass. Towards lower electron densities the dip in general decreases, in contrast to the calculations, which predict dips between about 0.35 for $N_e = 10^{17}$ cm^{-3} and greater than 0.5 at our lowest electron densities. (Doppler and instrumental broadening are taken into account.) These dip values are out of scale in Fig. 9.

In order to determine the effective reduced

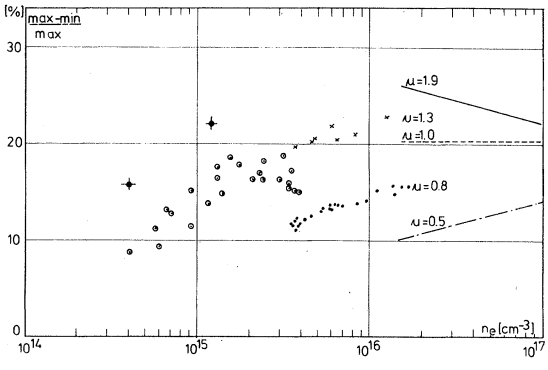

FIG. 9. Central dip of H_β vs electron density with the reduced mass as parameter. The straight lines represent the results of Kelleher and Wiese for reduced masses of $\mu = 0.5$ (H – H$^+$), 1.0 (H – A$^+$), and 1.9 (D – A$^+$). The present results for $\mu = 0.8$ (H – He$^+$) (symbols ● and ⊙) and $\mu = 1.3$ (D – He$^+$) (symbols ×, and +) are shown, too. The dip values indicated by × (μ = 0.8) and + ($\mu = 1.3$) were obtained in a 70-Torr helium arc, the dips at higher electron densities in a 1-atm helium arc, theoretical dips range from 35% ($n_e = 10^{17}$ cm^{-3}) to more than 50% at low electron densities; Doppler and instrumental broadening are taken into account.

mass, which has to be evaluated from the relative density of helium and hydrogen (deuterium) ions in the plasma, we observed the width of helium lines with and without the small admixture of hydrogen (deuterium) in the arc center. No significant change in the helium linewidth could be found to indicate a change in electron density and, thus, helium ions were always the dominant species of perturber ions in our plasma.

At an electron density of 3.5×10^{15} cm^{-3} in Fig. 9, the arc pressure changes from 1 atm to 70 Torr. This reduction of the arc pressure produces an increase of the H_β dip from 11.5% to about 16% at fixed electron density and reduced mass. In the Table II we have put together all physical quantities which may produce the observed effect (see also Fig. 5).

In the following we discuss in detail the influence of these quantities.

(a) Changes in neutral-atom density. While the electron density remains unchanged, the density of neutral atoms changes considerably. Since Van der Waals broadening is negligible in comparison to Stark broadening, we can discount the neutral-atom effects.

(b) Electron temperature. The quasistatic-ion theories predict an increase of the dip with increasing electron temperature, but only about 5% as compared with 28% for the jump in electron temperature stated in Table II. There is no evidence for such a strong dependence of the dip on electron temperature in the experimental data either; e.g., in the Kelleher-Wiese experiment[15] no change in the H_β dip is observed at approximately fixed electron density and reduced mass in an argon and neon arc, the electron temperature in the latter being considerably higher.[39] Thus, only a small portion of the dip increase can be attributed to the increase of the electron temperature.

(c) Gas temperature. The difference in Doppler broadening due to the jump in the gas temperature is less than 1% of the H_β half-width and accounts for a relatively small portion of the observed difference in the dips associated with the two temperatures. Most of the increase in the dip can be related to the decrease of the gas (atom-ion) temperature, i.e., to ion-dynamic effects. This behavior is consistent with the reduced mass dependence of the dip, since one would expect from the mean velocity between radiator and perturbing ion,

$$v=(8kT_g/\pi\mu)^{1/2}, \tag{7}$$

and increase of the H_β dip with increasing reduced mass and decreasing gas temperature, if ion motion relative to the emitting atom is responsible for the observed discrepancies between experiment and theory. In this consideration the quasistatic calculations have the character of a limiting case for $v=0$.

Inspection of Fig. 9 shows that at an electron density of 2×10^{16} cm^{-3} dip values for five different reduced masses are available. Kinetic temperatures range from $1-2\times10^4$ K for the electrons and from about 1 to 1.5×10^4 K for the ions. In the earlier arc experiment,[15] the H_β dip was observed to scale as $1/\sqrt{\mu}$ for a fixed electron density and at approximately the same electron and gas temperature. In Fig. 10 we have plotted all dips obtained at $N_e=2\times10^{16}$ cm^{-3} vs $(T_g/\mu)^{1/2}$, i.e., the mean relative atom-ion velocity. In this representation the dips measured in this experiment lie somewhat above the straight line through the Kelleher-Wiese results. This can be related to the quite different electron temperatures of $T_e\approx2\times10^4$ and $T_e\approx10^4$ K respectively, in the two experiments. If our measured dips at $T_e\approx2\times10^4$ K are adjusted to $T_e\approx10^4$ K, assuming the calculated dependence of the dip on the electron temperature[1,2] to be valid, the obtained values fall on the straight line through the data for $T_e\approx10^4$ K (crosses in Fig. 10). This suggests a good agreement between experimental and theoretical dependence of the H_β dip on the electron temperature. Extrapolation of the dips to the static case by assuming a linear dependence of the dips on the mean ion-atom velocity (for an approximately fixed electron tem-

TABLE II. Variation of H_β "dip" with temperature.

Arc Pressure (Torr)	760	70	Change (%)
Electron density (cm^{-3})	3.5×10^{15}	3.5×10^{15}	
Reduced mass	0.8	0.8	
Dip (%)	11.5	≈16	+28
Electron temperature (K)	17 500	20 000	+12.5
Gas temperature (K)	10 200	8 100	−20.6
Stark width (FWHM)	4.4 Å	4.4 Å	
Van der Waals (FWHM)	0.08 Å	0.008 Å	
Doppler (FWHM)	0.35 Å	0.31 Å	

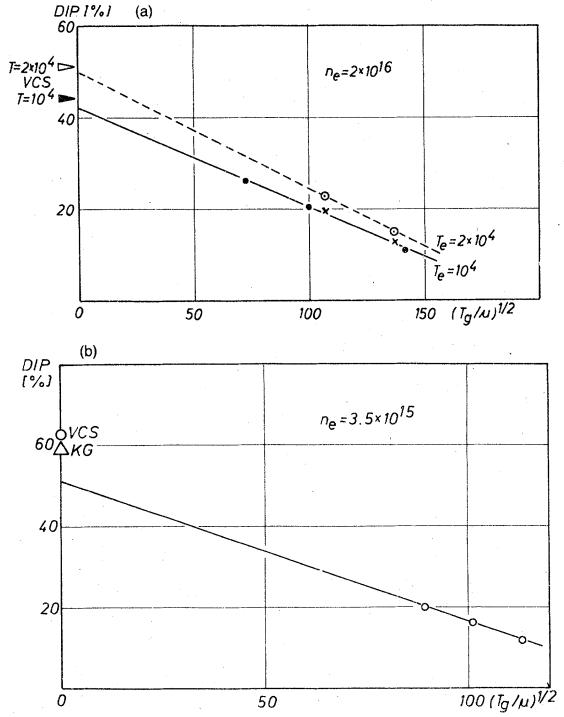

FIG. 10 (a). Central H_β minimum vs $(T_g/\mu)^{1/2}$. ●, Kelleher-Wiese experiment ($T_e = 10^4$ K); ⊙, this experiment ($T_e = 2\times10^4$ K); ×, this experiment, T_e corrected to 10^4 K according to the calculated T_e dependence of the H_β dip. Linearly extrapolated values to the static case are in good agreement with the VCS dip values for both temperatures (the KG values are only slightly smaller). Central H_β minimum vs $(T_g/\mu)^{1/2}$ at $N_e = 3.5\times10^{15}$ cm^{-3}.

perature) yields surprisingly good agreement with the quasistatic calculations for both electron temperatures. The VCS dip values are marked in Fig. 10 (the KG values are slightly smaller).

The above treatment only considers a single radiator- (ion) perturber pair. Hey and Griem[10] point out the many-body nature of this problem: the line centers are formed by small field strengths which are produced by many ions rather than a single perturber. Though this fact makes our results even more surprising, a purely accidental agreement of the extrapolated values with the calculations seems rather unlikely.

At an electron density of approximately 10^{15} cm^{-3} we have compared our measured H_β and D_β profiles with recent calculations by Cooper, Smith, and Vidal (CSV),[23] which include ion-motion effects. The "unified" theory utilized in both the VCS[2] and CSV[23] calculations does not make the completed collision ("impact") approximation. Within the limits of its other approximations (e.g., binary strong collisions and neglect of time-ordering effects associated with the rotation of the perturbing electric field with respect to the atomic dipole), the theory is valid over the full range of interaction time scales from the impact to the quasistatic regime. The VCS and CSV calculations differ in that the VCS calculations treat only the electrons according to the unified theory (ions are treated as quasistatic), while CSV treat both electrons and ions in a "unified" way. This second treatment has a very limited range of validity, since the unified theory assumes that all strong collisions are binary. The interaction time with an atom is of course much longer for a slow-moving ion that it is for an electron, and it turns out that strong atom-ion collisions are isolated in time only for electron densities below about 10^{15} cm^{-3} at our experimental temperatures.

The authors (CSV) have provided us with extensive unpublished tables of their results, which allowed us to generate a profile for our experimental electron density and reduced mass, and to convolve the Stark profile with the Doppler profile corresponding to our experimental gas temperature. It was not possible to circumvent the assumption made by CSV that $T_i = T_e$, and in our plasma these two temperatures were quite different. However, most of the temperature dependence of the CSV profiles appear to be correlated to the electron temperature (this can be seen by comparision with the VCS profiles, which assume that $T_i = 0$). The dependence of the CSV profiles on T_i is apparently very weak, as it is on the reduced mass. While this is not in qualitative agreement with our measured results, it does mean that the profile in Fig. 11 corresponding to the CSV calculation ($T_e = T_i = 17\,000$ K) is probably quite similar to that which would be calculated at our experimental conditions ($T_e = 17\,000$ K, $T_i = 4500$ K). Both theoretical profiles in Fig. 11 have been convolved with a Doppler profile corresponding to experimental conditions ($T_a = 4500$ K, instrument function width of 0.05 Å). Computed profiles have been normalized to have the same half-width and peak height as the measured ones; the experimental profiles are an average of the red and blue side (see Fig. 8).

Note the difference in the electron densities between CSV and VCS profiles having the same width; in a recent experiment[38] excellent agreement of the VCS calculations with an independently determined electron density is reported at an electron density of about 10^{15} cm^{-3}. A comparison of the profiles in Fig. 11 indicates that while the agreement of the measured H_β dip with the CSV calculation is better than with the VCS quasistatic-ion results, it is worse in the remainder of the profile. The measured ion-dynamic effects appear

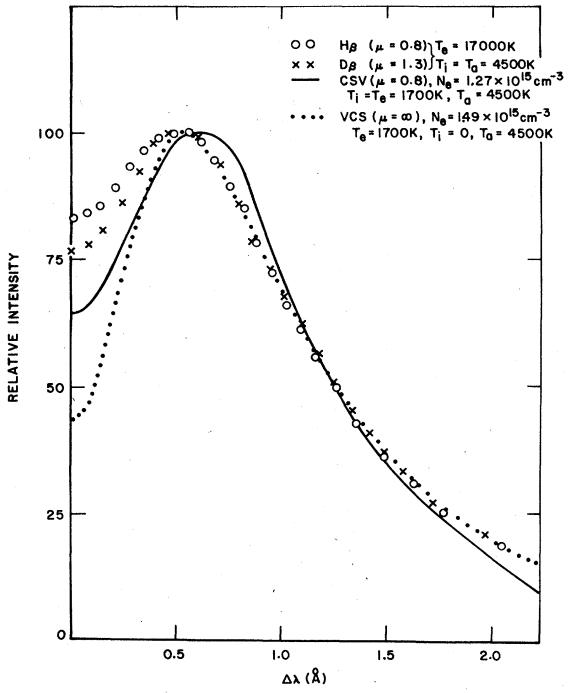

FIG. 11. Experimental H_β and D_β profiles as well as theoretical H_β profiles with (CSV) and without (VCS) ion dynamics. H_β and D_β profiles emitted simultaneously from the same plasma. The half-width of one line is about 1 Å, the asymmetry is due to overlapping of the line wings. The central minimum of D_β is much more pronounced than that of H_β.

to affect only the region very close to line center, within the H_β maxima.

Calculations have been performed[40-42] which include the nonadiabatic effect of the rotation of the ion-electric-field vector with respect to the atomic dipole. In this theory, an attempt is also made to account for many-body effects by considering an effective net rotation; the main limiting approximation is the expansion of the time-dependent electric field to second order, which is valid only if ion-dynamic effects are small. Computed values for the H_β dip agree reasonably well with measured ones, although the scaling of μ^{-1} is in disagreement with the experimental one of $\mu^{-1/2}$.

Calculations based on the "model microfield method"[43-49] (MMM) can be made in a straightforward way to include ion-motion effects. The method approximates the actual electric microfield with a series of "kangaroo processes" (KP). The vector field is constant over certain intervals, making sudden jumps between values. The time-averaged distribution of the field amplitude is weighted according to the quasistatic microfield probability distribution. The intervals between jumps have a Poisson distribution, except that the characteristic jumping frequency "ν" is not a constant; rather it is made to depend on the field strength in such a way that the autocorrelation function of the KP field is equal to that of the actual time-dependent field. The solution to the Schrödinger equation with KP fields can be found exactly in the semiclassical approximation. The time-dependent fields of both the electrons and ions can be taken into account simultaneously, and there is no need for the questionable process of convolving the electron and ion profiles.

A complete and rigorous justification of the MMM is still lacking.[46] However, Seidel[48] has recently demonstrated the remarkable fact that the MMM calculations for the electrons agree almost perfectly with the unified-theory results (including time ordering). The existing experimental vindication is also impressive, particularly in the central region of hydrogenic lines where the binary theories generally break down when the ions are included. Though some discrepancies still persist, particularly at low electron densities, agreement with the core of measured H_α and H_β profiles is quite good.[45,49] Also, the first-order corrections for ion-dynamical corrections turn out to be proportional to the relative ion-atom velocity, in agreement with experiment. [This has been shown by Brissaud and Mazure[45] by expanding Eq. (17) of Ref. 46 to first order in $\nu(E)$, the KP frequency.] Finally, a MMM calculation[49] for L_α which includes dynamical-ion contributions predicts a total width that is twice as large as calculated when the ions are treated quasistatically,[1,2] in agreement with the recent experimental result of Grützmacher and Wende.[50]

Measurements by Burgess and Mahon[16] for the same electron density and reduced mass (0.8), but a gas and electron temperature of 10^4 K (this experiment, $T_g = 4500$ K) yield a dip of at most 4% (this experiment, ≈15%). This result is *qualitatively* consistent with our observed dependence of the H_β dip on the gas temperature.

In two recent experiments the central region of H_β has been investigated at electron densities near 10^{15} cm^{-3}. Evans, Aeschliman, and Hill[38] obtained H_β profiles by means of a hydrogen-seeded argon-plasma jet for $T_e = 10^4$ K and $T_g = 6000$ K, while Ramette and Drawin[17] observed the H_β profile in the afterglow of a Z-pinch discharge in the temperature range 5000–3500 K. In comparison to our profiles, relatively strong asymmetries enhancing the blue peak over the red one and smaller H_β dips are observed in both experiments, indicating possible homogeneity problems (see Fig. 2). In the case of the afterglow plasma, the authors observed spectral features in the line core and line wings, which are believed to be caused by ion and

electron plasma waves, respectively. Our measured profiles do not show any indications of those structures, but the conditions in our stationary light source may be rather different from those in a transient plasma.

Finally it should be noted that the static Stark-effect pattern of H_β exhibits a small unshifted central component at low-field strengths (electron densities), if fine-structure (spin) effects are included in the calculations.[51] This fact should contribute to the filling in of the H_β dip at very low electron densities.

(iii) H_γ. Figure 12 shows a measured H_γ profile, obtained at an electron density of 1.1×10^{15} cm^{-3} in comparison to a theoretical profile calculated by VCS (the KG profile is very similar). Both profiles are area normalized to unity, the far wings of the experimental profile are assumed to follow a $\Delta\lambda^{-5/2}$ slope. No asymmetry could be found in the measured profile. As can be seen in Fig. 12, the calculated profile exhibits a pronounced "shoulder," produced by the unshifted central Stark component superimposed on a "background" of the shifted components. As with H_α and H_β, less structure is observed near the line center than predicted theoretically; the shoulder is outlined only weakly in the measured H_γ profile. With respect to the calculated profile, intensity in the experimental profile is mainly transferred from the very line center to the nearby wavelength region, filling in the theoretically predicted shoulders. This behavior is quite similar to that observed in the H_α line center, indicating again that there may be some problems with the unshifted Stark components in the calculations. Within our experimental-error bars, which are mainly due to uncertainties in electron density, the remainder of the calculated profile below the shoulder is in good agreement with our measured profile. Particularly at low electron densities, the absence of a pronounced shoulder in the experimental profiles give rise to significant discrepancies between theoretical and experimental half-widths of H_γ. This situation is shown in Fig. 13, where the ratios of the measured as well as calculated (VCS) H_γ and H_β half-widths are plotted versus electron density. While the experimental ratio is nearly constant, the VCS ratio decreases towards low electron densities; towards higher densities this ratio tends to approach the experimental value.

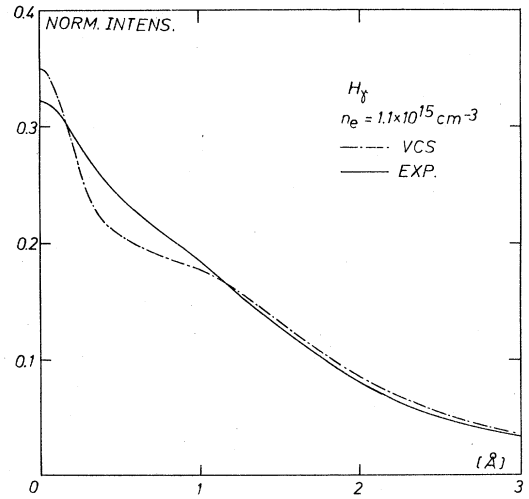

FIG. 12. Experimental and theoretical H_γ profiles for T_e = 16 500 K and T_g = 4000 K. The profiles are area normalized; Doppler and instrumental broadening are taken into account in the VCS profile. (The KG profile is very similar.)

III. CONCLUSIONS

Measurements of the plasma broadening of the Balmer lines H_α, H_β, and H_γ in the electron-density range between approximately 4×10^{14} and 2×10^{16} cm^{-3} have yielded the following main results.

(i) The measured line shapes show less structure in the line centers than predicted by theories based on the quasistatic approximation for the ions. These discrepancies increase towards low electron densities, and become very large for H_α. At a fixed electron density the overall agreement in the line center between experiment and theory improves with increasing principal quantum number of the upper state.

(ii) The central minimum of H_β was found to depend inversely on the square root of the reduced mass in the radiator- (ion) perturber system. Also, our data indicate that the H_β dip depends on the gas temperature in such a way that the H_β dip appears to depend linearly on the mean relative velocity between radiator and perturber. Extrapo-

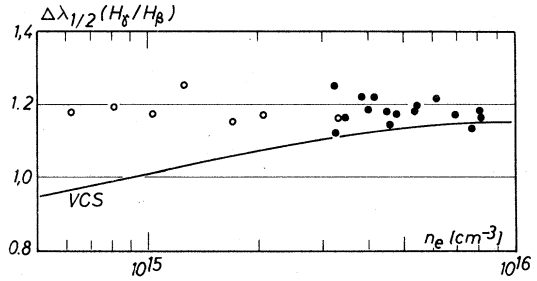

FIG. 13. Ratio of the H_γ and H_β half-widths vs electron density. O, ●, : experimental values for the 70-Torr and 1-atm arc, respectively. Doppler and instrumental broadening are taken into account in the theoretical (VCS) linewidth ratio.

lation to the static case gives good agreement with dips calculated by quasistatic-ion theories. Recent calculations[23] including ion-dynamic effects show improved agreement with the experimental H_β line center, but the agreement with the half-width and the remainder of the profile is degraded. Other calculations[40-42] indicate the nonadiabatic effects due to electric-microfield rotation are important. Model microfield calculations[45,49] are apparently in quite good agreement with experiment.

The H_β-D_β "twins," which were spectrally resolved in the same plasma, show clearly that the reduced mass dependence of these profiles is not produced by instabilities or similar phenomena. Ion-dynamic effects can account for a considerable part of the observed discrepancies in hydrogen line centers. The dependence of the H_α (and possibly H_γ) as well as H_β line centers on ion dynamics indicate that ion-dynamic corrections to the line broadening should not be restricted to the field-strength distribution,[10] because these corrections do not affect the unshifted central Stark components. This, as well as other theoretical investigations, has yielded no significant ion-dynamic effect up to now in case of H_β.[20]

(iii) At the lower end of our investigated electron-density range ($\lesssim 10^{15}$ cm^{-3}), a considerable part of the observed discrepancies in the H_α line center can be attributed to the neglect of fine-structure (spin) effects in the calculations; also, a part of the filling in of the H_β dip should be due to this effect.

ACKNOWLEDGMENTS

We wish to thank Dr. W. L. Wiese for many helpful discussions and suggestions. One of us (H.E.) would like to thank Dr. W. L. Wiese for his hospitality and the Deutsche Forschungsgemeinschaft for the support during his stay at the National Bureau of Standards. We are also grateful to Dr. J. Cooper for several fruitful discussions and for providing us with the unpublished tables of the CSV profiles. Thanks as well to Dr. J. F. Delpech and A. Phelps for useful discussions on the collisional problems.

---

*Permanent address: Institut für Experimentalphysik, Olshausenstr. 40-60, 2300 Kiel, W. Germany.

[1](a) P. Kepple and H. R. Griem, Phys. Rev. 173, 317 (1968). (b) H. R. Griem, *Spectral Line Broadening by Plasmas* (Academic, New York, 1974).
[2]C. R. Vidal, J. Cooper, and E. W. Smith, Astrophys. J. Suppl. 25, 37 (1973).
[3]W. L. Wiese, D. E. Kelleher, and D. R. Paquette, Phys. Rev. A 6, 1132 (1972).
[4]E. A. McLean and S. A. Ramsden, Phys. Rev. 140, 1122 (1965).
[5]R. A. Hill and J. B. Gerardo, Phys. Rev. 162, 45 (1967).
[6]R. A. Hill and E. H. Beckner, Appl. Opt. 3, 929 (1964).
[7]R. A. Hill, J. B. Gerardo, and P. Kepple, Phys. Rev. A 3, 855 (1971).
[8]J. C. Morris and R. U. Krey, Phys. Rev. Lett. 21, 1043 (1968).
[9]H. Ehrich and H. J. Kusch, Z. Naturforsch. 28a, 1794 (1973).
[10]J. D. Hey and H. R. Griem, Phys. Rev. A. 12, 169 (1975).
[11]J. B. Shumaker, Jr. and C. H. Popenoe, Phys. Rev. Lett. 21, 1046 (1968).
[12]K. Behringer, Z. Phys. 246, 333 (1971).
[13]B. Wende, Z. Naturforsch. 22a, 181 (1967).
[14]W. L. Wiese, D. E. Kelleher, and V. Helbig, Phys. Rev. A 11, 1854 (1975).
[15]D. E. Kelleher and W. L. Wiese, Phys. Rev. Lett. 31, 1431 (1973).
[16]D. D. Burgess and R. Mahon, J. Phys. B 5, 1756 (1972).
[17]J. Ramette and H. W. Drawin, Z. Naturforsch. 31a, 401 (1976).
[18]H. Ehrlich and D. E. Kelleher, Phys. Rev. A 17, 1686 (1978).
[19]L. J. Roszman, Phys. Rev. Lett. 34, 785 (1975).
[20]R. W. Lee, J. Phys. B 6, 1060 (1973).
[21]E. R. A. Segre and D. Voslamber, Phys. Lett. A 46, 397 (1974).
[22]D. Voslamber, Phys. Lett. A 61, 27 (1977).
[23]J. Cooper, E. W. Smith, and C. R. Vidal, J. Phys. B 7, L101 (1974).
[24]H. Maecker and S. Steinberger, Z. Angew. Phys. 23, 456 (1968).
[25]W. L. Wiese, in *Methods of Experimental Physics*, edited by B. Bederson and W. L. Fite (Academic, New York, 1968), Vol. 7A, p. 307.
[26]J. Uhlenbusch and G. Gieres, Z. Agnew. Phys. 27, 66 (1969).
[27]A. J. Barnard, J. Cooper, and E. W. Smith, J. Quant. Spectrosc. Radiat. Transfer 14, 1025 (1974).
[28]H. R. Griem, *Plasma Spectroscopy* (McGraw-Hill, New York, 1964).
[29]D. E. Kelleher, thesis, Univ. of Maryland, 1977 (unpublished).
[30]W. L. Wiese, in Proceedings of the Seventh Yugoslavia Symposium on the Physics of Ionized Gases, 1974 (unpublished).
[31]H. W. Drawin, Phys. Lett. A 42, 423 (1973).
[32]A. Unsöld, *Physik der Sternatmosphären* (Springer-Verlag, Berlin, 1955).
[33]H. S. W. Massey and E. H. S. Burhop, *Electronic and Ionic Impact Phenomena* (Oxford University, London, 1952), p. 229.

[34]M. Glass Maujean, J. Phys. B. 11, 431 (1978); Comments At. Mol. Phys. 7, 83 (1977).
[35]M. Gryzinski, Phys. Rev. 115, 379 (1959).
[36]E. W. McDaniel, *Collision Phenomena in Ionized Gases* (Wiley, New York, 1964), Chap. 1.
[37]C. H. Muller, thesis, University of Colorado, 1976 (unpublished).
[38]D. L. Evans, D. P. Aeschliman, and R. A. Hill, Phys. Rev. A 10, 2430 (1974).
[39]J. Uhlenbusch, E. Fischer, and J. Hackmann, (unpublished); T. Aachen, Z. Phys. 239, 120 (1970); 238, 404 (1970).
[40]G. V. Sholin, V. S. Lisitsa, and V. I. Kogan, Sov. Phys. JETP 32, 758 (1971).
[41]A. V. Demura, V. S. Lisitsa, and G. V. Sholin, in Proceedings of the 12th International Conference on the Phenomena of Ionized Gases, Eindhoven, 1975. (unpublished), p. 37.
[42]A. V. Demura, V. S. Lisitsa, G. V. Sholin, Sov. Phys. JETP 73, 400 (1977).
[43]U. Frisch and A. Brissaud, J. Quant. Spectrosc. Radiat. Transfer 11, 1753 (1971).
[44]A. Brissaud and U. Frisch, J. Quant. Spectrosc. Radiat. Transfer 11, 1767 (1971).
[45]A. Brissaud and A. Mazure (unpublished).
[46]A. Brissaud, C. Goldbach, J. Léorat, A. Mazure, and G. Nollez, J. Phys. B; 9, 1129 (1976).
[47]A. Brissaud, C. Goldbach, J. Léorat, A. Mazure, and G. Nollez, J. Phys. B; 9, 1147 (1976).
[48]J. Seidel, Z. Naturforsch. 32a, 1195 (1977).
[49]J. Seidel, Z. Naturforsch. 32a, 1207 (1977).
[50]K. Grützmacher and B. Wende, Phys. Rev. A 16, 243 (1977).
[51]G. Lüders, Ann. Phys. 8, 301 (1951).